Energy Research Journal 1 (2): 120-125, 2010
ISSN 1949-0151

Photocatalytic Activity and Antibacterial Behavior of Fe^{3+}-Doped TiO_2/SnO_2 Nanoparticles

[1,2]Lek Sikong, [2]Budsabakorn Kongreong, [3]Duangporn Kantachote and [1,2]Weerawan Sutthisripok
[1]NANOTEC Center of Excellence at Prince of Songkla University, Thailand
[2]Department of Mining and Materials Engineering, Faculty of Engineering,
[3]Department of Microbiology Science, Faculty of Science,
Prince of Songkla University, Songkhla, Thailand

Abstract: Problem statement: Since bacteria mainly causes damage on fresh vegetables and fruits during transportation to market, anti-bacterial TiO_2 photocatalyst was applied for their packaging films. However, it has been known that pure TiO_2 exhibits low photocatalytic property due to rapid recombination of photo-activated electrons and holes. Doping with metal or metal oxide shows the improvement of photocatalytic activity and disinfection effect. **Approach:** Fe^{3+} was considered to dope into $TiO_2/3SnO_2$ photocatalyst in order to enhance the photocatalytic property and bacterial inactivation efficiency. The Fe^{3+} doped $TiO_2/3SnO_2$ nanoparticles were prepared by sol-gel method and calcined at 400 °C for 2 h. The synthesized powders were characterized by XRD, BET and SEM. Photocatalytic activity and bacteria killing effect were determined by means of degradation of methylene blue solution and inactivation of *E. coli* bacteria, respectively. These tests were performed under UV and visible light irradiations. **Results:** Fe^{3+} doping into $TiO_2/3SnO_2$ has an effect on inhibition of anatase crystal growth, led to the enlargement of the composite specific surface area. Therefore, the photocatalytic activity of Fe^{3+} doped $TiO_2/3SnO_2$ composite in proper concentration was greater than those of pure TiO_2 and $TiO_2/3SnO_2$ and 0.5 mol% Fe^{3+} doping exhibited the highest photocatalytic activity and *E.coli* inactivation efficiency. The *E. coli* was completely killed within 90 min under UV irradiation or 99.7% inactivated under visible light exposure. **Conclusion:** Fe^{3+} doped $TiO_2/3SnO_2$ nanoparticles were successfully synthesized and identified as 100% anatase phase. The 0.5mol% Fe^{3+}-doped $TiO_2/3SnO_2$ which has particle size of 12.89 µm and specific surface area of 117.61 $m^2 g^{-1}$, exhibited the highest activity and disinfection efficiency. An attractive feature of Fe^{3+} doped $TiO_2/3SnO_2$ photocatalytic disinfection is its potential to be activated by visible light. Therefore, these composite TiO_2 nanoparticles can be utilized for fresh food packaging films.

Key words: Photocatalytic, sol-gel, antibacterial, Fe^{3+} doped TiO_2/SnO_2, TiO_2

INTRODUCTION

In recent years, titanium dioxide has been extensively used as an environmentally harmonious and clean photocatalyst, because of its various qualities, such as optical properties, low cost, high photocatalytic activity, chemical stability and non-toxicity (Hoffmann *et al*., 1995; Fujishima *et al*., 2000). However, its practical application seems limited for several reasons, among which one is the low photon utilization efficiency; another is the need to use the Ultraviolet (UV) as an excitation source. In order to solve these problems, the modification of these catalysts has also been attempted by doping them with various transition metals, including Fe^{3+}. Because the experimental conditions, preparation methods and standards for the evaluation of photocatalytic activity are there are many argumentative results reported. Some research groups have reported that the presence of these foreign metal species in TiO_2 is generally detrimental for the degradation of organic compounds in aqueous systems (Paola *et al*., 2000; Navio *et al*., 1999; Dohshi *et al*., 2003; Sinha *et al*., 2001) while some controversial results have also been reported (Choi *et al*., 1994; Zhang *et al*., 1998; Yamashita *et al*., 2002; Araña *et al*., 2002). The photocatalytic sterilization property of Titanium dioxide (TiO_2) has been documented (Watanabe *et al*., 1999). The first research on the microbiocidal effect of TiO_2 photocatalytic reactions was carried out with

Corresponding Author: Lek Sikong, Department of Mining and Materials Engineering,
Faculty of Engineering, Prince of Songkla University, Songkhla, Thailand

Escherichia coli (Matsunaga *et al*., 1985) and subsequently has been intensively conducted on a wide spectrum of organisms including viruses, bacteria, fungi, algae and cancer cells (Sinha *et al*., 2001) In the last decade, TiO_2 has been widely utilized as a self-cleaning and self-sterilizing material for coating many clinical tools including sanitary ware, food tableware and cooking ware and items for use in hospitals (Fujishima *et al*., 2000). It has been approved by the American Food and Drug Administration (FDA) for use in human food, drugs and cosmetics and compounded in food contact materials such as cutting board and other surfaces in contact with unprotected food. An anticipated use as a new material technology for future requirements is in the hygienic design of food processing facilities. As known, doping TiO_2 with metallic ions or oxides such as Fe^{3+}, Ag, or SnO_2 enhances the photocatalytic activity and bacteria killing effect (Zhang *et al*., 2008; Akhavan, 2009; Erkan *et al*., 2006).

In this study presents the effect of Fe^{3+} doped in $TiO_2/3SnO_2$ photocatalyst on TiO_2, crystallite size, photocatalytic reaction and bacteria disinfection.

MATERIALS AND METHODS

Raw material: Titanium (IV) isoproxide (TTIP, 99.95%, Fluka Sigma-Aldrich), tetrachlorostannane pentahydrate ($SnCl_4.5H_2O$) and ferric chloride anhydrous ($FeCl_3$) were used as starting materials. Ethanol (99.9%; Merck Germany) was used as a solvent.

Sample preparation: The $TiO_2/3SnO_2$ doped Fe^{3+} (0.3, 0.5, 0.8, 1.0, 1.2 mol%) powders were prepared via a conventional sol-gel method (Fig. 1).

Firstly, TTIP was dissolved in ethanol, mixed with $SnCl_4.5H_2O$ and $FeCl_3$ by stirring for 15 min at room temperature and followed by adding droplets of 4 M NH_3 into the solution until pH about 3-4. Finally, distilled water was slowly added to the solution by stirring for 30 min. The solution was dried at 105°C for 24 h and calcined at the temperature 400°C for 2 h. The synthesized powder was ground and submitted to determine the particle size by a light scattering particle analyzer before using as a photocatalyst.

Materials characterization: The phase identification of samples was conducted with X-ray diffraction analysis using X-ray diffractometer (PHILIP X'Pert MPD). The crystallite size was determined from XRD peaks using the Scherer equation (Bakardjieva *et al*., 2005):

$$D = 0.9\lambda/\beta\cos\theta_B \quad (1)$$

When:

D = Crystallite size (nm)

λ = the wavelength of the x-ray radiation (CuKα = 0.15406 nm)

β = the angle width at half maximum height

θ_B = the half diffraction angle of the centroid of the peak in degree

The morphology of sample and specific surface area of $TiO_2/3SnO_2/0.5Fe^{3+}$ powder were characterized by Scanning Electron Microscope (SEM), Matersizer 2000 and BET surface area measurement, respectively.

Photocatalytic reaction test: The photocatalytic activity was evaluated by the degradation of methylene blue (MB) under UV (310-400 nm wave length) irradiation using four 50 W black light lamps. A 400 ml MB with a concentration of 1×10^{-5} M was mixed with 1.5 g of photocatalytic powders (pure TiO_2, $TiO_2/3SnO_2$ and $TiO_2/3SnO_2$ doped with 0.3, 0.5, 0.8, 1.0 and 1.2 mol% Fe^{3+}) under UV irradiation for 0, 15, 30, 45, 60, 75 and 90 min. After photo-treatment for a certain time, the concentration of treated solution was measured by Ultraviolet-Visible spectrophotometer (UV-Vis).

The percentage of degradation of MB is calculated by:

$$\text{Percentage of degradation} = 100(C_0\text{-}C)/C_0 \quad (2)$$

When:

C_0 = the concentration of MB aqueous solution at beginning (1×10^{-5} M)

C = the concentration of MB aqueous solution after exposure

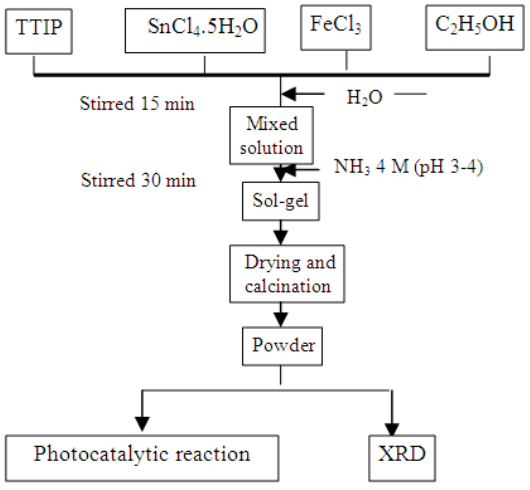

Fig. 1: Preparation produce of $TiO_2/3SnO_2$ doped Fe^{3+} (0.3, 0.5, 0.8, 1.0, 1.2 mol%) by so-gel method

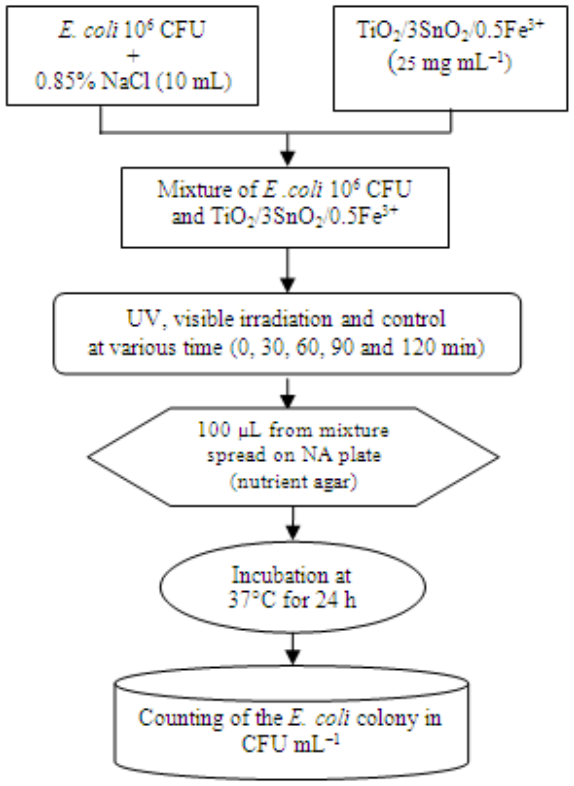

Fig. 2: Photocatalytic reaction test of $TiO_2/3SnO_2/0.5Fe^{3+}$ powder against *E. coli*

Photocatalytic reaction of $TiO_2/3SiO_2/0.5Fe^{3+}$ powder against *E. coli*: Figure 2 shows the procedure of photocatalytic reaction in antibacterial activity of $TiO_2/3SnO_2/0.5Fe^{3+}$ powders against *E. coli*. Aliquots of 10 mL *E. coli* conidial suspension were mixed with 250 mg of $TiO_2/3SnO_2/0.5Fe^{3+}$ powders. The mixture was then exposed to irradiation of UV and visible light at various times (0, 30, 60, 90 and 120 min). Then, 1 mL of mixture suspension was sampled, added to the Nutrient Agar (NA) plate and incubated at 37°C for 24 h. After incubation, the number of viable colonies of *E. coli* on each NA plate was observed. The control experiment (*E. coli* + catalyst at 37°C without light) was also performed.

RESULTS

Characterization: Particle size and surface area of $TiO_2/3SnO_2/0.5Fe^{3+}$ powder after calcination at 400°C and ground by using mortar were 12.89 µm (Fig. 4 and Table 2) and 117.61 m^2 g^{-1}, respectively. It was found from Fig. 4 that the agglomeration of synthesized composite powders was observed. Fig. 3 shows XRD patterns of Fe^{3+} - doped $TiO_2/3SnO_2$ powders calcined at 400°C for 2 h. All samples have shown similar peaks with the highest peak at 25.3° which was indicated as 100% anatase phase. The crystallite size of Fe^{3+}-doped $TiO_2/3SnO_2$ with 0.3, 0.5, 0.8, 1.0 and 1.2 mol% Fe^{3+} were 18.46, 16.53, 20.59, 16.52 and 18.44 nm, respectively (Table 1). This result shows the Fe^{3+} doping in range of 0.3~1.2% mol exhibits nearly the same crystallite size of anatase phase.

Photocatalytic properties of Fe^{3+}-doped $TiO_2/3SnO_2$ nanopowders: The photocatalytic activity of Fe^{3+}-doped $TiO_2/3SnO_2$ powders were evaluated by photocatalytic decolorzation of MB aqueous solution.

Table 1: Crystallite size and phases of $TiO_2/3SnO_2/Fe^{3+}$ powders synthesized at various Fe^{3+} contents after calcination at 400°C for 2 h

Fe^{3+} content (mol%)	Crystallite size (nm)		Phase content (%)	
	Anatase	Rutile	Anatase	Rutile
0.3	18.46	-	100	0
0.5	16.53	-	100	0
0.8	20.59	-	100	0
1.0	16.52	-	100	0
1.2	18.44	-	100	0

Table 2: Particle size of $TiO_2/3SnO_2/Fe^{3+}$ synthesized ground powders

Fe^{3+} content (mol%)	Particle size (µm)
0.3	15.75
0.5	12.89
0.8	12.10
1.0	14.36
1.2	14.23

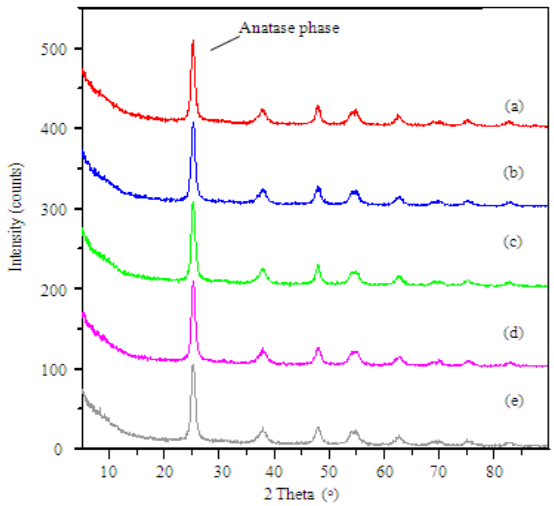

Fig. 3: XRD patterns of Fe^{3+}-doped $TiO_2/3SnO_2$ powders prepared by sol-gel method and calcined at 400°C for various Fe^{3+} contents, (a) 0.3 mol% Fe^{3+}; (b) 0.5 mol% Fe^{3+}; (c) 0.8 mol% Fe^{3+}; (d) 1.0 mol% Fe^{3+} and (e) 1.2 mol%Fe^{3+}

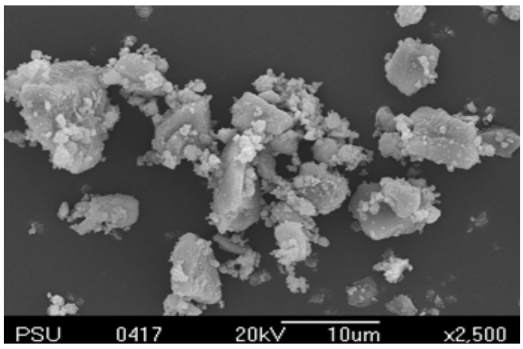

Fig. 4: SEM image of 0.5 Fe^{3+}-doped $TiO_2/3SnO_2$ powder prepared by sol-gel method and calcined at 400°C for 2 h

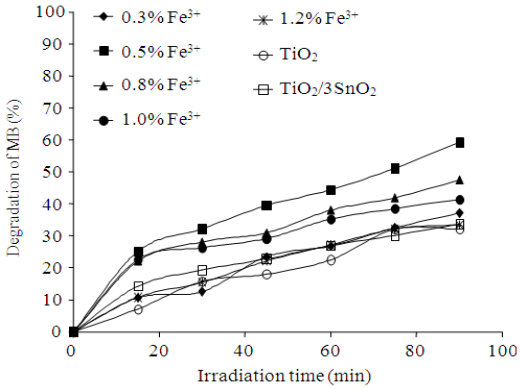

Fig. 5: The degradation effect of MB plotted against irradiation time for pure TiO_2, $TiO_2/3SnO_2$ and $TiO_2/3SnO_2$ doped with 0.3, 0.5, 0.8, 1.0 and 1.2 mol% Fe^{3+} photocatalysts

Figure 5 shows the degradation of MB solution using Fe^{3+}-doped $3SnO_2$/ TiO_2 powders, pure TiO_2 and SnO_2-doped TiO_2 powders under UV light for 15 min until 90 min.

The degradation effect of MB by Fe^{3+}-doped $TiO_2/3SnO_2$ in some concentrations of Fe^{3+} was better than those of pure TiO_2 and $TiO_2/3SnO_2$. After 90 min of testing, the percent degradation was 32.0, 33.6, 37.1, 59.3, 47.5, 41.5 and 33.5 when using pure TiO_2, $TiO_2/3SnO_2$ and $TiO_2/3SnO_2$ doped with 0.3, 0.5, 0.8,1.0 and 1.2 mol% Fe^{3+} respectively (Fig. 5). It was found that $TiO_2/3SnO_2/0.5Fe^{3+}$ showed the best activity in degradation of MB and hence it was selected for antibacterial activity test.

Results of $TiO_2/3SnO_2/0.5Fe^{3+}$ photocatalysis against *E. coli*: The viable colonies of *E. coli* on NA plates with the presence of $TiO_2/3SnO_2/0.5Fe^{3+}$ powder under UV, visible light and control conditions are shown in Fig. 6.

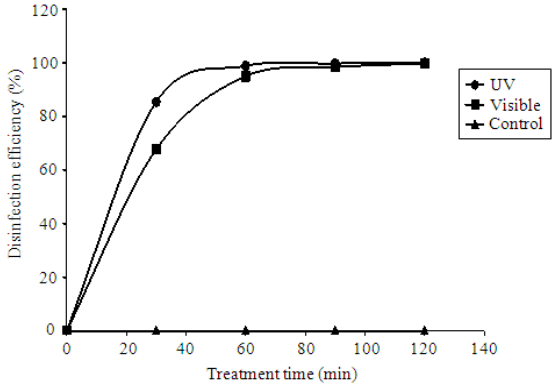

Fig. 6: The photocatalytic *E. coli* disinfection efficiency of $TiO_2/3SnO_2/0.5Fe^{3+}$ plotted against treatment time under UV, visible light irradiation and control

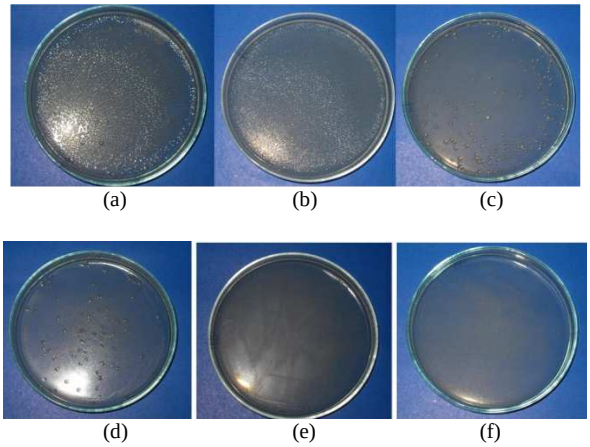

Fig. 7: Growth of *E. coli* on Nutrient Agar (NA) plate with the presence of $TiO_2/3SnO_2/0.5Fe^{3+}$ under UV irradiation or visible light and control, (a) control at starting time; (b) control treatment at 90 min; (c) after visible light irradiation time for 30 min; (d) after UV irradiation for 30 min; (e) after visible light irradiation for 90 min and (f) after UV irradiation for 90 min

The number of viable colonies of *E. coli* when added $TiO_2/3SnO_2/0.5Fe^{3+}$ and exposed to UV and visible light decreased with increasing time as shown in Fig. 7 while control environment (*E. coli* + $TiO_2/3SnO_2/0.5Fe^{3+}$ without light) had not changed (Fig. 7b). It was found that with the presence of $TiO_2/3SnO_2/0.5Fe^{3+}$, *E. coli* was completely inactivated within 90 min under UV irradiation as shown in Fig. 7f and under whereas the percent degradation has reached 99.7% when exposed to visible light for 90 min (Fig. 7e).

Figure 6 shows the disinfection efficiency curve plotted against photo-treatment time. It was found that the disinfection efficiency increased rapidly at first 30 and 60 min for UV and visible light treatment, respectively and after that they slightly increased and approached to 100% with increasing time.

DISCUSSION

It was apparent that Fe3+ doping has an effect on hindrance of anatase crystal growth, therefore the crystallite sizes of $TiO_2/3SnO_2/0.5Fe^{3+}$ nanoparticles (16~20 nm) are smaller than those of pure TiO_2 (33 nm) and undoped $TiO_2/3SnO_2$ (25 nm). This leads to enhancement of photocatalytic activity and disinfection efficiency due to their larger specific surface area. $TiO_2/3SnO_2/0.5Fe^{3+}$ nanomaterials have demonstrated strong antimicrobial properties through a mechanism including photocatalytic production of reactive oxygen species that damage cell components and viruses (Li *et al*., 2008). As the results, an attractive feature of $TiO_2/3SnO_2/0.5Fe^{3+}$ photocatalytic disinfection is its potential to be activated by visible light or sun light. Therefore, these composite TiO_2 nanoparticles will be utilized for fresh food packaging films.

CONCLUSION

- Fe^{3+} doped $TiO_2/3SnO_2$ nanoparticles were successfully synthesized and identified as 100% anatase phase. The 0.5mol% Fe^{3+}-doped $TiO_2/3SnO_2$ particle size and surface area was 12.89 μm and 117.61 $m^2 g^{-1}$, respectively
- The photocatalytic degradation of methylene blue in aqueous solution of Fe^{3+} doped $TiO_2/3SnO_2$ powder at 0.5% mol Fe^{3+} under UV irradiation exhibited higher activity compared to other concentrations
- $TiO_2/3SnO_2/0.5Fe^{3+}$ nanopowder showed excellent photocatalytic activity under both UV and visible light irradiation towards *E. coli* inactivation
- With the presence of $TiO_2/3SnO_2/0.5Fe^{3+}$, *E. coli* was completely inactivated within 90 min irradiation in UV light or 99.7% inactivated under visible light exposure

ACKNOWLEDGEMENT

This research has been supported by Department of Mining and Materials Engineering, Faculty of Engineering and Department of Microbiology Science, Faculty of Science, Prince of Songkla University. Special thanks regards to Prince of Songkla University fund and NANOTEC Center of Excellence at Prince of Songkla University to provide the budget for this research.

REFERENCES

Akhavan, O., 2009. Lasting antibacterial activities of Ag-TiO_2/Ag/a-TiO_2 nanocomposite thin film photocatalysts under solar light irradiation. J. Colloid Interface Sci., 336: 117-124. DOI: 10.1016/J.JCIS.2009.03.018

Araña, J., G. Díaz, S.M. Miranda, J.M. Doña Rodríguez, J.A. Herrera Melián and J. Pérez Peña, 2002. Maleic acid photocatalytic degradation using Fe-TiO_2 catalysts: Dependence of the degradation mechanism on the Fe catalysts content. Applied Catal. B: Environ., 36: 113-124. DOI: 10.1016/S0926-3373(01)00284-3

Bakardjieva, S., J. Šubrt, V. Štengl, M.J. Dianez and M.J. Sayagues, 2005. Photoactivity of anatase-rutile TiO_2 nanocrystalline mixtures obtained by heat treatment of homogeneously precipitated anatase. Applied Catal. B: Environ., 58: 193-202. DOI: 10.1016/J.APCATB.2004.06.019

Choi, W., A. Termin and M.R. Hoffmann, 1994. The role of metal-ion dopants in quantum-sized TiO_2: correlation between photoreactivity and charge-carrier recombination dynamics. J. Phys. Chem., 98: 13669-13679. DOI: 10.1021/j100102a038.

Dohshi, S., M. Takeuchi and M. Anpo, 2003. Effect of the local structure of ti-oxide species on the photocatalytic reactivity and photo-induced super-hydrophilic properties of Ti/Si and Ti/B binary oxide thin films. Catal. Today, 85: 199-206. DOI: 10.1016/s0920-5861(03)00387-0.

Erkan, A., U. Bakir and G. Karakas, 2006. Photocatalytic microbial inactivation over Pd doped SnO_2 and TiO_2 thin films. J. Photochem. Photobiol. A: Chem., 184: 313-321. DOI: 10.1016/J.JPHOTOCHEM.2006.05.001.

Fujishima, A., T.N. Rao and D.A. Truk, 2000. Titanium dioxide photocatalysis. J. Photochem. Photobiol. C: Photochem. Rev., 1: 1-21. DOI: 10.1016/S1389-5567(00)00002-2.

Hoffmann, M.R., S.T. Martin, W. Choi and D.W. Bahnemann, 1995. Environmental Applications of Semiconductor Photocatalysis. Chem. Rev., 95: 69-96. DOI: 10.1021/cr00033a004

Li, Q., S. Mahendra, D.Y. Lyon, L. Brunel and M.V. Liga *et al*., 2008. Antimicrobial nanomaterials for water disinfection and microbial control:Potential applications and implications. Water Res., 42: 4591-4602. DOI: 10.1016/j.watres.2008.08.015

Matsunaga, T., R. Tomoda, T. Nakajima and H. Wake, 1985. Photoelectrochemical sterilization of microbial cells by semiconductor powders. FEMS Microbiol. Lett., 29: 211-214. DOI: 10.1111/j.1574-6968.1985.tb00864.x

Navio, J.A., J.J. Hidalgo, M. Roncel and M.A. Dela Rosa, 1999. A laser flash photolysis study of the photochemical activity of a synthesized $ZrTiO_4$: Comparison with parent oxides, TiO_2 and ZrO_2. Mater. Lett., 39: 370-373. DOI: 10.1016/s0167-577x (99)00037-3

Paola, A.D., G. Marci, L. Palmisano, M. Schiavello, and K. Uosaki *et al*., 2000. Preparation of polycrystalline TiO_2 photocatalysts impregnated with various transition metal ions: Characterization and photocatalytic activity for the degradation of 4-nitrophenol. J. Phys. Chem. B., 106: 637-645. DOI: 10.1021/jp013074l

Sinha, S., T. Murugesan, K. Maiti, J.R. Gayen, B. Pal and M. Pal *et al*., 2001. Antibacterial activity of bergenia ciliata rhizome. Fitoterapia, 72: 550-552. DOI: 10.1016/s0367-326x(00)00322-1

Watanabe, T., A. Nakajima, R. Wang, M. Minsabe and S. Koizumi *et al*., 1999. photocatalytic activity and photoinduced hydrophilicity of titanium dioxide coated glass. Thin Solid Films, 351: 260-263. DOI: 10.1016/S0040-6090(99)00205-9

Yamashita, H., M. Harada, J. Misaka, M. Takeuchi and K. Ikeue *et al*., 2002. Degradation of propanol diluted in water under visible light irradiation using metal ion-implanted titanium dioxide photocatalysts. J. Photochem. Photobiol. A: Chem., 148: 257-261. DOI: 10.1016/S1010-030(02)00051-5

Zhang, Z., C. Wang, R. Zakaria and J.Y. Ying, 1998. Role of particle size in nanocrystalline TiO_2-based photocatalysts. J. Phys. Chem. B., 102: 10871-10878. DOI: 10.1021/jp982948+

Zhang, W., Y. Chen, S. Yu, S. Chen and Y. Yin, 2008. Preparation and antibacterial behavior of Fe^{3+}-doped nanostructured TiO_2 thin films. Thin Solid Films, 516: 4690-4694. DOI: 10.1016/J.TSF.2007.08.053